

Survey For Ruin Like Formations On The Moon

Alexey V. Arkhipov

rai@ira.kharkov.ua

Institute of Radio Astronomy, 4 Krasnoznamenaya str., Kharkov, 61002, **Ukraine**

ABSTRACT

As a continuation of preliminary analysis of Clementine lunar images [2], an automated computer survey for ruin-like objects on the Moon has been executed. The finds are now classified and catalogued. It is shown that majority of these formations could be interpreted as collapsed subsurface cavities. Such local formations are puzzling from a geological perspective, and seem promising candidates for archaeological objects. Besides, such subsurface cavities in Polar Regions could be interesting for other reasons, such as colonization of the Moon or as lava tubes.

1. INTRODUCTION

Our thesis is that the Moon could be used as indicator of extraterrestrial intelligence (ETI) visits to our unique "alive" planet [1]. ETI, as well as NASA, could understand the strategic significance of Moon-ports for interplanetary communications. That is why it is reasonable to search for alien artifacts (e.g. ETI bases of 0-4 Gyr age) on our satellite.

Various computer algorithms were proposed and tested for the archaeological reconnaissance of the Moon [2]. About 20,000 Clementine lunar orbital HIRES images have been processed, and a few ruin-like formations were found. Now the results of similar automated survey of all HIRES polar images (~80,000 files) are presented.

2. SURVEY AND CATALOGUE

As in the preliminary search, the orbital images of high-resolution camera (HIRES, 9-30 m/pixel) of the Clementine space probe [3] were analyzed. Only the polar lunar regions of $\pm 75^\circ$ to $\pm 90^\circ$ latitudes were processed in this survey because of their oblique lighting. Basic tests used for image selection are described in [2]. These are the preliminary fractal, rectangular, geological tests and the SAAM filter. Moreover, two new tests were added.

1. The false alarm probability was decreased by discarding of excessively shadowed images (shadow filter). If $>5\%$ of pixels are dimmer than 10% of the maximum brightness amplitude, that image was ignored. Files of <13 KB size were discarded too.

2. For filtering of shadow interference after the preliminary fractal test, the

following "FREX" procedure was used. The fractal a-parameter (a measure of artificiality) was computed as in [2], but for only 1 of every 5 points to speed up the analysis of the images. The average linear regression relating to the random image set and zenith angle of the Sun (Z_{sun}) was calculated by this simple algorithm. If the image was lower than the a- Z_{sun} regression minus 1/2 of its standard deviation, the image was selected.

In summary, the preliminary fractal test, shadow filter, FREX and rectangular tests selected ~5% of the images as interesting. The selected files were SAAM filtered and tested visually. About 97% of the selections were ignored after SAAM testing. The remaining 128 finds are catalogued (see Table I). Only 47 catalogued images were still selected after the geological test. Their orientations are different (>10 deg.) from the significant directions of background lineaments (details in [2]). Finally, only 18 files of these 47 were selected as most interesting after the full fractal test for artificiality. Their a-factors deviate from a- Z_{sun} regression for 100 random images by more than 3 times of its standard deviation. Such images of top interest are marked by asterisks in Table I.

However, it is not reasonable to ignore other catalogued finds. Human activity, for example, correlates with geological lineaments (e.g. valleys, rivers, deposits around faults). That is why a negative result of geological test is not evidence of natural object; but a positive result would be an additional argument for POSSIBLE artificiality. Moreover, eroded objects could be of low contrast on images taken from orbit. Their fractal properties might be insufficiently different from background. Hence, the fractal test could undervalue the find. That is why all finds in Table I are of potential interest for archaeological reconnaissance of the Moon.

The finds in the catalogue are described as systems of simple quasi-rectangular elements: d - depressions; f - furrows; h - quadrangle hills; p - rectangular pattern of craterlets; r - ridges. Thus, an abbreviation such as "dr" in the last column of Table I means "a system with quasi-rectangular depression(s) and quasi-rectangular ridges". This method of description is convenient for morphological analysis.

3. MORPHOLOGY AND PHENOMENOLOGY

There are two main types of ruin-like formations.

1. Quasi-rectangular patterns of depressions (recdeps). About 69% of ruin-like finds could be attributed to this type. Usually recdep is a cluster of rectangular depressions with rectangular ridges between them. This wafer pattern may be seen in the examples shown in Fig. 1.

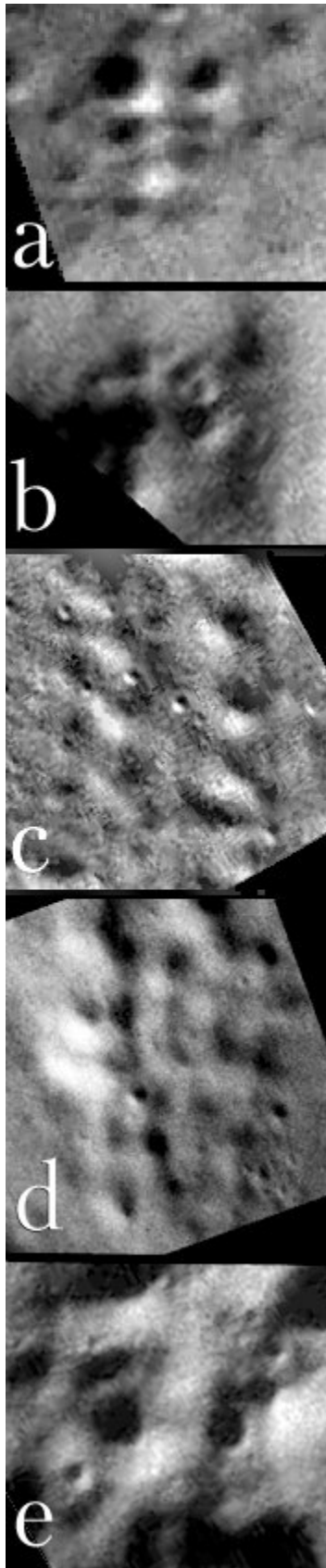


Figure 1

"Recdep" examples in evolutionary order: (a) LHD0316A.083; (b) LHD0470B.112; (c) LHD5443Q.291; (d) LHD5472Q.287; (e) LHD5661R.068.

Presumably, an isolated, single rectangular depression could be considered as an extreme form of recdep. Moreover, there are transitional forms from rectangular pattern of craterlets to recdep (e.g. Fig. 1b). So, recdeps in the Table I have descriptions with d, dr or p elements. The typical size of recdeps is ~1-3 km. The size of these rectangular depressions is 0.1-2 km. Quasi-rectangular patterns of depressions correlate with plain terrains (e.g., inter-crater space, or the bottom of the large-scale craters).

2. Quasi-rectangular lattices of lineaments (reclats). These comprise 30% of the ruin-like formations here. A reclat is a complex of interlacing, broken ridges or furrows, which form the quasi-rectangular pattern (Fig. 2).

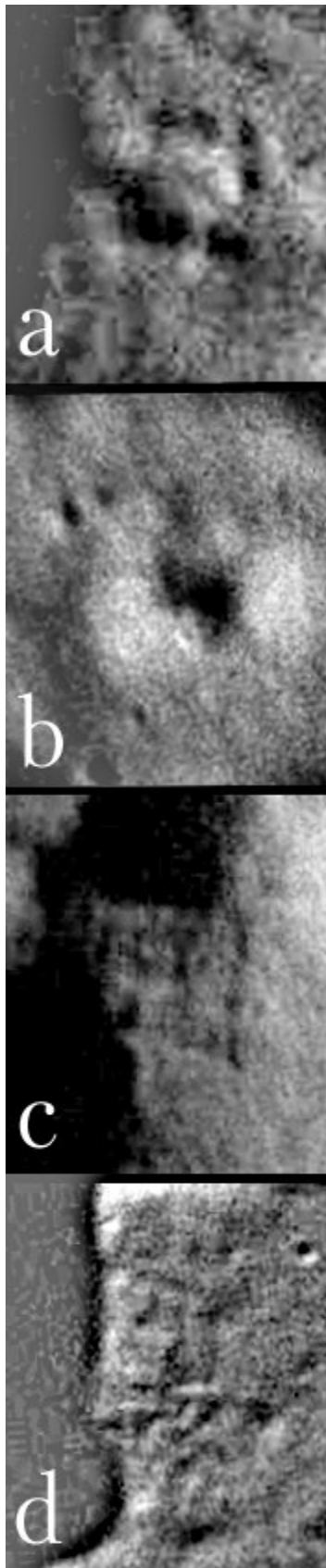


Figure 2

"Reclats" examples in evolutionary order: (a) LHD0558B.072; (b) LHD5559Q.279; (c) LHD6749R.318; (d) LHD6158R.320.

This morphological type is present in Table I as complexes of r and/or f elements without d. These lineaments have a typical width of ~50 m and cover territory of ~1 km. Reclats correlate with slopes and hill tops, where the regolith layer must be thinnest. Apparently, what we see is subsurface structure rather than some organization of regolith.

Besides recdeps and reclats, quadrangle hills are worthy of separate description. The hills are located in formations of both morphological types. The dimensions of such hills are 0.3-1 km. Usually the quadrangle hill has a craterlet on its top. Sometimes the top depression is so large that the hill appears hollow (Fig. 3).

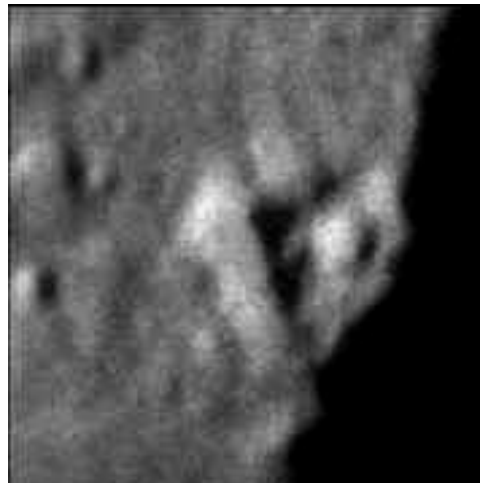


Figure 3

The hollow hill is bounded by a rectangular depression: a candidate for embankment (LHD5345Q.059).

The rectangular depressions around the hill on Fig. 3 are a rarity for the Moon, but they are common for man-made mounds on the Earth.

4. INTERPRETATIONS

The origin of ruin-like formations could be reconstructed from images of various stages of their evolution.

Thus, the reconstruction of recdep evolution is shown in Fig. 1. The simplest, probably the first stage formation, is a regular pattern of craterlets (Fig. 1a). Apparently, this is the collapse or regolith drainage into subsurface caverns. Expanding craterlets became angular. The rectangular lattice of ridges appears between them (Fig. 1b). The rectangular lineaments around such formation (Fig. 1c) show the regular and local nature of subsurface caverns. Such a cavern system is seen after its total collapse (Fig. 1d). The bottom collapses (Fig. 1e) and slope terraces [1] in rectangular depressions argue for several levels of caves.

The reclat evolution could be interpreted in terms of erosion too (Fig. 2). Apparently, the first (simplest) stage of reclat is the quasi-rectangular system of narrow

furrows-cracks (Fig. 2a). The cracks expand (Fig. 2b) and transform into quasi-rectangular pattern of ridges (Fig. 2c). The Fig. 2d shows the quadrangle mesa-like hill surrounded by the ridge system (using the high-pass filter of Adobe Photoshop). Obviously, such ridges are a relatively stable aspect of the hill they reside on.

These rectangular systems of depressions and ridges resemble terrestrial ruins. Recdeps and reclats are too localized and regularized for tectonic features or jointing pattern of impacts. Subsurface, rectangular, multilevel caves are not known in lunar geology. However, they are usual considered in modern plans for lunar bases. The rectangular systems of ridges could be interpreted in terms of archaeology too. Of course, suggesting this possibility is not a form of evidence, but rather an argument for archaeological reconnaissance in situ.

5. CONCLUSIONS

The systematic survey for lunar ruin-like objects is realized. The results follow.

1. New ruin-like formations are found.
2. A catalogue of promising objects for archaeological reconnaissance of the Moon is compiled. Even if catalogued finds are natural, they are interesting examples of unusual lunar geology.
3. Catalogued rectangular systems of depressions and ridges (recdeps and reclats) are landscape forms not described in other catalogues.
4. It is argued that recdep could be interpreted as a collapse of a subsurface system of caves. Such rectangular, multilevel caverns could be interesting for archaeology, geology and sites for lunar base.

Therefore, the archaeological reconnaissance of the Moon appears to be a viable, active, interdisciplinary field of science.

ACKNOWLEDGEMENTS

The author is grateful to Dr. Y.G.Shkuratov for access to the Clementine CDs. I also thank Dr. L.N.Litvinenko and Dr. T. Van Flandern for support.

REFERENCES

1. A.V. Arkhipov, "Earth-Moon System as a Collector of Alien Artifacts", J. Brit. Interplanet. Soc., 51, 181-184 (1998).
2. A.V. Arkhipov, Preliminary Search For Ruin-Like Formations on the Moon, Meta Research Bulletin, 8, No. 4, 49-54.
3. DoD/NASA, "Mission to the Moon", Deep Space Program Science Experiment, Clementine EDR Image Archive. Vol. 1-88. Planetary Data System & Naval Research Laboratory, Pasadena, 1995 (CDs).

Table. Catalogue of Ruin-Like Finds

Note: The central coordinates of images are in degrees. The last column contains the quasi-rectangular elements (see text for definitions).

Table I. CATALOGUE OF RUIN-LIKE FINDS

Longitude	Latitude	File	Elements
deg.	deg.		
11.05	89.16	LHD5814R.295	d
13.63	85.57	LHD5741R.295	d
16.08	-76.10	LHD0480B.030	f
* 20.03	-81.24	LHD0395A.160	p
20.69	-79.70	LHD0159B.293	dr
22.50	80.63	LHD5686R.160	r
25.38	75.50	LHB5443Q.291	prf
28.25	-76.50	LHD0132B.290	dr
* 28.35	79.10	LHD5502Q.290	f
31.16	80.78	LHD5833R.157	f
* 31.21	78.82	LHD5256Q.293	d
32.97	79.60	LHD5538Q.289	f
33.55	77.27	LHD5715Q.156	dr
33.57	77.05	LHD5713Q.156	dr
35.45	81.20	LHD5555R.289	rfd
37.00	77.58	LHD5472Q.287	pr
37.18	79.86	LHD5525Q.287	df
41.93	-82.88	LHD0280A.151	fd
43.09	86.94	LHD5724R.286	dr
44.05	-75.87	LHD0445B.151	r
51.34	-83.68	LHD0233A.147	f
* 53.95	-83.54	LHD0287A.146	rd
56.88	87.01	LHD5705R.282	dr
60.29	79.20	LHD5559Q.279	d
60.30	85.14	LHD5636R.280	p
108.97	-76.82	LHD0412B.127	rhf
109.85	-82.38	LHD0344A.126	d
113.40	82.50	LHD5350R.260	fdr
123.50	86.07	LHD5652R.126	df
124.55	-82.47	LHD0282A.121	d
128.05	80.00	LHD5375R.254	?
128.25	-78.26	LHD0162B.253	f
128.41	-76.13	LHD0191B.253	r
128.83	82.91	LHD5459R.254	dr
130.26	-82.91	LHD0073A.252	d
130.33	-82.75	LHD0274A.119	rp
130.52	79.32	LHD4691Q.253	pf
130.71	80.68	LHD4722R.253	dr

131.20	-78.77	LHD0111B.252	dr
135.66	80.05	LHD4807R.251	?
137.97	-84.74	LHD0276A.116	dr
139.41	-86.30	LHD0184A.115	f
145.91	77.84	LHD5288Q.247	f
148.00	-81.36	LHD0248A.113	f
148.41	-79.04	LHD0305B.113	d
149.69	-84.26	LHD0231A.112	f
150.71	-81.43	LHD0315A.112	rd
151.29	-77.99	LHD0415B.112	d
151.44	-76.24	LHD0470B.112	pr
154.36	83.95	LHD6979R.244	p
155.35	83.91	LHD5605R.112	dp
156.86	83.25	LHD5564R.243	f
159.68	-78.18	LHD0343B.109	pr
164.46	76.18	LHD4993Q.240	rf
164.51	81.34	LHD5173R.240	fd
166.93	89.03	LHD5643R.114	dr
167.15	80.91	LHD5286R.239	f
169.86	81.35	LHD5175R.238	d
169.87	79.18	LHD5107Q.238	dr
171.02	-81.44	LHD0095A.238	p
* 179.43	89.72	LHD5696R.248	fp
190.15	-77.39	LHD0469B.098	rf
191.53	83.32	LHD5417R.230	pr
* 191.54	83.21	LHD5416R.230	r
192.67	-80.56	LHD0308A.097	r
* 192.83	-81.40	LHD0096A.230	dr
* 192.90	-76.89	LHD0392B.097	f
197.24	89.46	LHD5611R.108	drf
200.20	78.82	LHD5279Q.227	dr
224.67	-76.57	LHD0421B.085	dr
224.72	-86.21	LHD0175A.083	r
229.10	-80.45	LHD0316A.083	p
230.32	-83.27	LHD0516A.082	pd
* 232.01	-76.20	LHD0210B.215	f
232.08	86.83	LHD5588R.217	fr
242.82	87.26	LHD5629R.214	df
243.37	82.05	LHD5628R.080	dr
244.03	-81.12	LHD0146A.210	d
244.99	85.05	LHD7605R.344	r
* 246.08	81.88	LHD7638R.343	fh
246.21	-82.25	LHD0142A.209	dr
* 250.58	-85.48	LHD0193A.073	r
251.14	-82.54	LHD0140A.207	r
251.65	79.76	LHD5397Q.209	f

254.56	79.99	LHD5250Q.208	f
254.65	-80.58	LHD0148A.206	r
258.78	-77.45	LHD0558B.072	f
* 261.17	86.87	LHD5466R.208	dr
* 266.18	-83.86	LHD0278A.068	r
266.42	86.58	LHD5492R.206	dr
268.33	87.79	LHD5595R.207	fp
* 269.63	85.11	LHD5650R.072	d
269.77	87.47	LHD5521R.206	dr
* 272.70	82.72	LHD5562R.202	r
273.41	79.55	LHD5545Q.069	d
273.56	79.74	LHD5547Q.069	d
281.47	-82.36	LHD0273A.063	fd
284.08	87.80	LHD5717R.202	dr
289.90	-80.94	LHD0149A.193	d
290.49	87.58	LHD5661R.068	d
291.22	-75.94	LHD0211B.193	d
292.29	77.16	LHD5116Q.194	d
292.30	77.07	LHD5110Q.194	d
293.74	-80.73	LHD0315A.059	p
296.28	-79.60	LHD0173B.191	dr
297.82	84.15	LHD5528R.193	dr
* 300.02	79.68	LHD5345Q.059	hd
300.98	80.42	LHD5441R.191	d
301.21	80.96	LHD5456R.191	dr
* 301.28	85.55	LHD6749R.318	r
301.55	-86.03	LHD0082A.320	h
301.58	-88.19	LHD0119A.052	r
* 306.10	-77.54	LHD0387B.055	dr
311.45	86.05	LHD6158R.320	rh
312.61	77.97	LHD5576Q.054	dr
312.73	78.18	LHD5578Q.054	dr
312.75	78.38	LHD5579Q.054	dr
314.96	77.38	LHD5307Q.053	dr
315.05	77.60	LHD5313Q.053	d
315.37	77.84	LHD5314Q.053	d
318.16	79.39	LHD5862Q.316	fdr
320.67	79.28	LHD5916Q.315	dr
323.28	86.62	LHD5574R.052	f
329.05	-78.41	LHD0362B.047	fd
338.05	86.90	LHD5972R.308	d
341.12	81.88	LHA3621R.307	dr
349.97	87.33	LHD5752R.303	pr
351.42	85.96	LHD5165R.171	r